



RESEARCH ARTICLE


Disease Spreading through Complex Small World Networks

H. E. Benítez^a, F. E. Cornes^a, C. O. Dorso^{a,b} and G. A. Frank^c

^a Departamento de Física, Facultad de Ciencias Exactas y Naturales, Universidad de Buenos Aires, Pabellón I, Ciudad Universitaria, 1428 Buenos Aires, Argentina.

^b Instituto de Física de Buenos Aires, Pabellón I, Ciudad Universitaria, 1428 Buenos Aires, Argentina.

^c Unidad de Investigación y Desarrollo de las Ingenierías, Universidad Tecnológica Nacional, Facultad Regional Buenos Aires, Av. Medrano 951, 1179 Buenos Aires, Argentina.

 OPEN ACCESS

PUBLISHED

30 September 2024

CITATION

Benítez, HE., Cornes, FE., et al., 2024. Disease Spreading through Complex Small World Networks. Medical Research Archives, [online] 12(9).

<https://doi.org/10.18103/mra.v12i9.5706>

COPYRIGHT

© 2024 European Society of Medicine. This is an open-access article distributed under the terms of the Creative Commons Attribution License, which permits unrestricted use, distribution, and reproduction in any medium, provided the original author and source are credited.

DOI

<https://doi.org/10.18103/mra.v12i9.5706>

ISSN

2375-1924

ABSTRACT

The end of the COVID-19 pandemic allows an analysis in retrospect of the spread and early containment scenarios of the disease. Today we can weigh the diversity of results imposed by highly heterogeneous urban landscapes (both geographical and social). In this research, we address scenarios of one or more communities (neighborhoods) formed by small structures with strong connectivity among themselves (families). Special attention was paid to the early containment of the epidemic. After simulating many scenarios, it was observed that early isolation of the infected individuals is more efficient than the isolation of their entire family. But we also noted that the containment of the disease loses effectiveness if the clinical tests for its detection are reported late (from 1 to 4 days). On the other hand, the existence of neighborhoods (with high population density) complicates the disease containment strategies, since (a) the disease spreads faster due to the highly dense environment, and (b) these act as “hubs of contagion”, even if the disease itself is of low contagiousness.

Keywords: complex networks, small world, COVID-19.

1. Introduction

Disease spreading along large population groups is a complex phenomenon since it depends on how individuals interact with each other and on the disease dynamics within each person. Both processes can vary from community to community¹⁻⁴ and the type of infectious agent⁵⁻⁷. This explains to some extent the wide range of observations seen during the COVID-19 pandemic in 2020⁸⁻¹¹.

Researchers observed that it's not possible to establish a self-consistent pattern of contagion among people unless considering their mobility. Mobility can create casual links between individuals who are not part of the family (or friends) environment^{2,5}. Studies on common mobility patterns suggest that these may vary according to the spatial scale under analysis¹². However, there exists a consensus in the literature that people follow a “scale-free” spatial distribution, within typical urban extensions¹³⁻¹⁶. Qualitatively speaking, this means that relatively few amount of individuals are responsible for the majority of social contacts, while the rest experience a more limited number of contacts¹⁷.

The mobility of individuals yields some kind of heterogeneity in the linking process of people within a network. For instance, some groups of people may exhibit higher densities of links than the commonly expected, thus, forming social “communities”. As a consequence, the epidemiological analysis has to be split into two scales: a “global” one concerning the overall evolution of the disease, and a “local” one concerning the evolution within a community¹⁸. This does not necessarily mean spatial scales, since the presence of specific “social layers” (which can overlap geographically) is also possible¹⁷.

Our investigation stands on the above perspective for the COVID-19 spreading. We organized the paper as follows:

- Section 2 presents a brief description of the working framework and the study design.
- Section 3 presents the results and discusses the investigation considering homogeneous networks, heterogeneous ones and mixed networks.
- Section 4 summarizes the main conclusions of the investigation.

2. Methods

The complexities mentioned in Section 1 motivate a microscopic approach to the epidemiological problem. This approach considers that each individual is somehow

immersed in an epidemiological environment similar to a “small world” network¹⁹. Within this context, each person may become infected and the disease evolves according to commonly accepted schemes described in the literature²⁰. We consider a four-stage (SEIR model) scheme for this investigation^{6,7}.

To acquire a precise insight into our microscopic approach, we organized this Section as follows:

- We first detail the framework of the investigation in Section 2.1. We introduce there our two major environments: the random and the scale-free networks (see Section 2.1.1). We also introduce a family structure for both environments in Section 2.1.2. The relevant features concerning these structures are detailed in Section 2.1.3. The epidemiological model is described in Section 2.1.4.
- The specific implementation of the above framework is detailed in Sections 2.2. This is divided for clarity reasons into the network implementation (Section 2.2.1) and the SEIR implementation (Section 2.2.2).

2.1 THE FRAMEWORK

2.1.1 Random and scale-free networks

A random network consists of N nodes connected by L links randomly distributed as detailed in ²¹. On the contrary, the scale-free network is built up in a somewhat sequential fashion, that is, linking one node at a time²². A new node to be linked is chosen randomly from the other m nodes already present in the network. The probability of connecting to any of these m nodes depends on the degree of the nodes²³. That is, for a node i of degree k_i , the connection probability reads as follows.

$$\pi(k_i) = \frac{k_i}{\sum_{j=0}^{N-1} k_j} \quad (1)$$

This type of connectivity is called preferential attachment²³. It yields a scale-free (or power law) probability distribution^{24,25}. Real-life examples for these networks are the Internet and human brain models^{26,27}.

Those nodes attaining a large number of links are commonly mentioned as *hubs* in the literature²⁴. The presence of *hubs* is of major relevance when comparing random and scale-free networks. Random networks achieve regular degrees k_i along the network. On the contrary, in scale-free networks, a few amount of nodes (*hubs*) are associated to a high degree, while many other nodes are associated to a low degree, say, a small number of links. Both kinds of networks are schematized in Fig. 1.

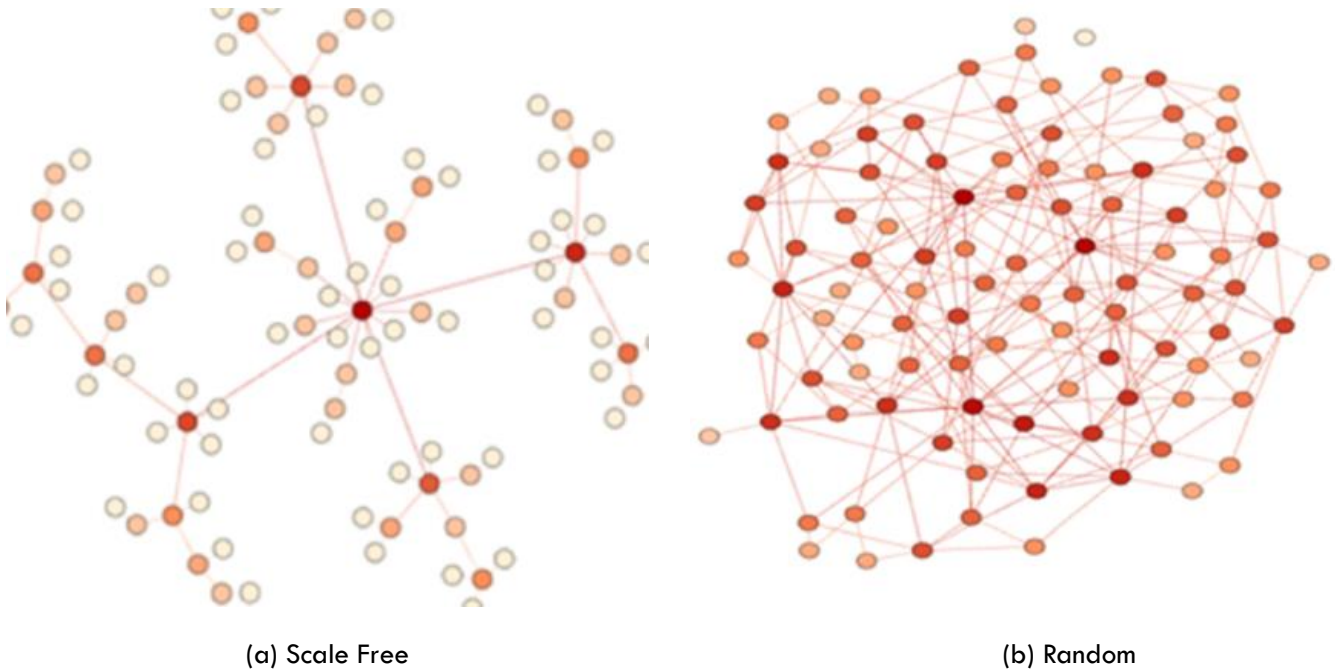


Figure 1. Examples of random and scale-free networks²⁸. The intensity of the colors indicates the degree of the node (the stronger the color, the higher the degree).

2.1.2 The Caveman Model

We choose the caveman model for representing either *intra* and *inter-family* interactions²⁹. Our caveman graph was built according to the following procedure: we first select 4 nodes randomly, (representing a family) and connect them to each other as a *clique*. Secondly, these

small groups or families are connected in a presumed fashion (see Fig. 2). Thus, all members of the same family interact with each other, but families may also interact with other families through connections resembling some kind of social structure. It is worth noting that all individuals are engaged in a family.

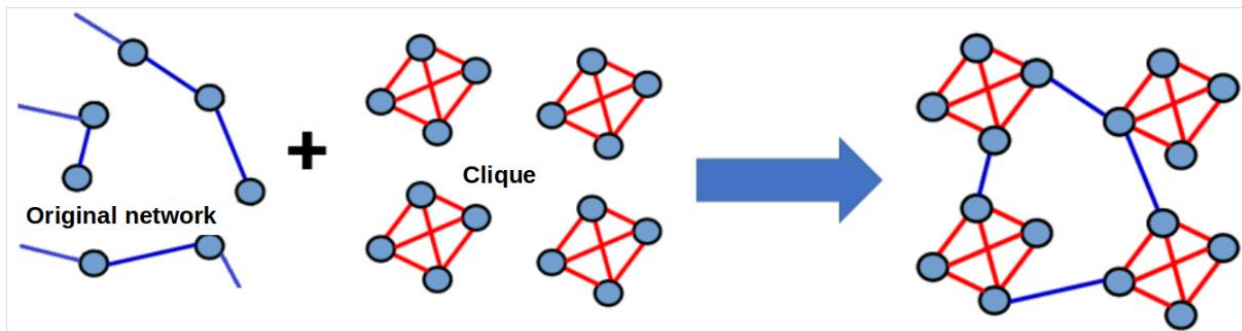


Figure 2. Scheme for a complex network attaining four families. The sub-graphs (families connected by red links) connect to the main network (blue links).

2.1.3 Betweenness, Modularity, and the Detection of Communities

The *betweenness* and *modularity* are key features in networks attaining community or neighborhood structures. Both are essential magnitudes in the detection of these structures. We now introduce a brief description of both magnitudes, and we next explain the procedure for detecting communities within the network.

The *betweenness* is the measure of how many times a node belongs to the shortest path between any two nodes of the network²⁵. For instance, in the network $G(N,L)$ built with N nodes connected by L links, the *betweenness* $CB(i)$ of the node i is defined as follows:

$$CB(i) = \sum_{j \neq k \in N} b_{ijk} / b_{jk} \tag{2}$$

where b_{ijk} means the number of shortest paths starting at node j and ending at k , but passing through node i . Accordingly, b_{jk} stands for the shortest path from node j to node k .

Fig. 3 displays an example of two communities represented in blue (squares) and green (circles) colors, respectively³⁰. Notice that node 1 holds the maximum *betweenness*, followed by node 22. Both nodes correspond to the most demanded ones along the network paths, and thus, its role in the network is somewhat crucial. On the contrary, the outermost nodes play a minor role in the network structure, and thus, are associated with an almost null *betweenness*.

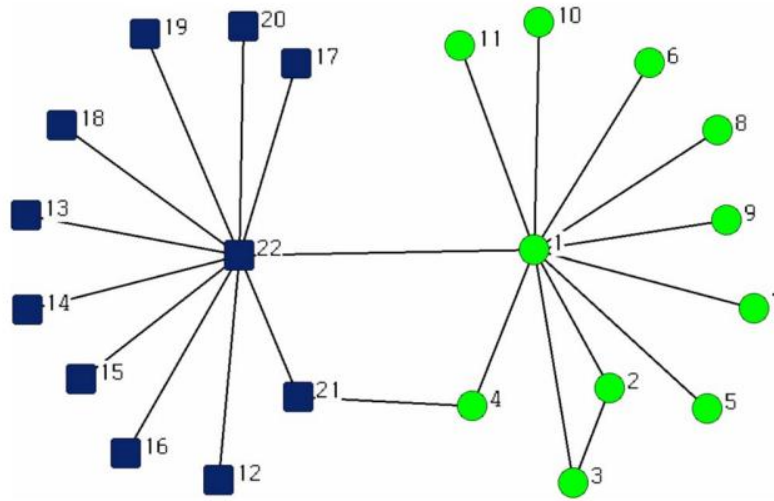


Figure 3. Example of a complex network with two communities colored in blue (squares) and green (circles), respectively. The link 22-1 achieves the highest value for the *betweenness*, followed by the link 21-4. The outermost links achieve the lowest values for the *betweenness*³⁰.

The *modularity* features the ease of splitting the network into communities (i.e. clusters). Consider, for instance, a network set up by N nodes and L links, but also composed of communities or clusters labeled as $c=1, \dots, n_c$. Each cluster is supposed to gather N_c nodes connected by means of L_c links. If L_c is larger than the expected number of links for the current link distribution, then this set of nodes (say, C_c) will be part of a potential community within the network. The *modularity* M features this belonging as follows.

$$M = \frac{1}{2L} \sum_{i,j \in C_c} \left(A_{ij} - \frac{k_i k_j}{2m} \right) \quad (3)$$

where A_{ij} represents the number of links between nodes i and j . k_i and k_j represent the degree of these nodes, while m corresponds to the total number of links in the network.

Any positive value of M means that C_c exceeds the expected number of links, and thus, is intended to form a community. The null condition $M=0$ stands for just a random connection among the N_c nodes. However, a negative value of M suggests that those nodes in C_c do not belong to a community²⁵.

Modularity is actually the key to recognizing communities. Those nodes achieving high values of M are found to be tightly connected to each other but loosely connected to the rest of the network.

The detection of communities, however, requires the computation of either the CB and M , as proposed by Girvan-Newman (GM)³¹. The GM algorithm starts with a single network and proceeds to compute CB and M . The nodes attaining the maximum *betweenness* are then identified. Next, the algorithm proceeds to eliminate the connection between these nodes²³, and immediately recomputes M . The procedure continues recursively, while the stage of maximum M is kept as the optimal identification.

2.1.4 The SEIR epidemiological model

The SEIR epidemiological model for the evolution of the disease is assumed throughout our investigation. This model considers that people belonging to a population of N individuals may be in any of the following compartmental stages:

- Susceptible $S(t)$: people who can become infected by contact with an infected person.
- Exposed $E(t)$: persons who carry the disease but can not yet infect others.
- Infected $I(t)$: individuals who carry the disease and can infect susceptible people in case they come into contact.
- Recovered or removed $R(t)$: persons who do not have the disease and are immune to it.

where $S(t)+E(t)+I(t)+R(t)=N$.

These basic compartments are a somewhat first approximation for the disease evolution. Many complex diseases may require more stages for a better description. However, we will focus on those cases where the SEIR model appears to be quite accurate.

We emphasize that unlike other epidemiological models (SIS, SIR, etc.), the SEIR model is well suited to the behavior of the COVID-19 Coronavirus epidemic. This is because this model includes individuals who carry the disease but, being in their incubation period for 5-6 days, are not able to infect other individuals⁷.

2.2 THE IMPLEMENTATION

In order to analyze the epidemiological dynamics of a “city”(i.e. community of a large number of people), two different contact networks were implemented: random and scale-free (preferential attachment)²². The random network is considered in our study as a reference, although scale-free networks better represent the social links in a city²².

We programmed low-level codes for either building the network and for implementing the SEIR temporal evolution. Statistics were computed from at least 30 realization of one million N nodes each. This kind of network is suitable for medium to big cities (say, Rosario or Mendoza in Argentina).

2.2.1 The Networks Implementation

Fig. 4 exemplifies the procedure for building a random network. In brief, the procedure starts with a set of N isolated nodes. The nodes are then linked randomly (with fixed probability). This mimics the casual contacts

between individuals, occurring with the same probability for all the individuals at any time.

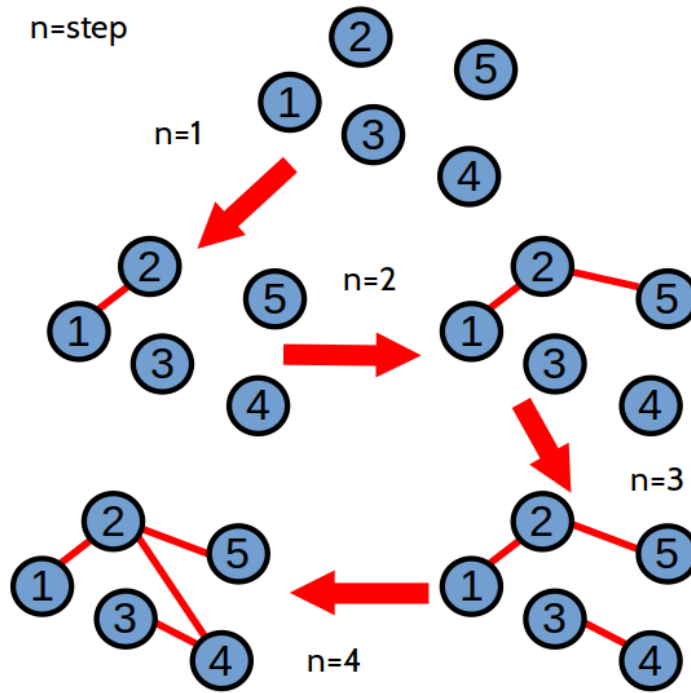


Figure 4. Procedure for building a random network (with 5 nodes). Node 1 is chosen and linked randomly to any other node. Then, node 2 is chosen and the process is repeated accordingly.

Fig.5 illustrates the procedure for the scale-free network (see caption for details). As a first difference with the random network, “new” nodes are now incorporated sequentially as follows:

1. Select a “new” node randomly.
2. Link the “new” node to an existing node i with associated probability $\pi(k_i)$ (see Eq. (1)).

3. Repeat the procedure until all the “new” nodes become connected.

This procedure ensures that a few nodes will achieve very high degree values. These were already mentioned as *hubs* in Section 2.1.1. Recall that *hubs* are not present in random networks.

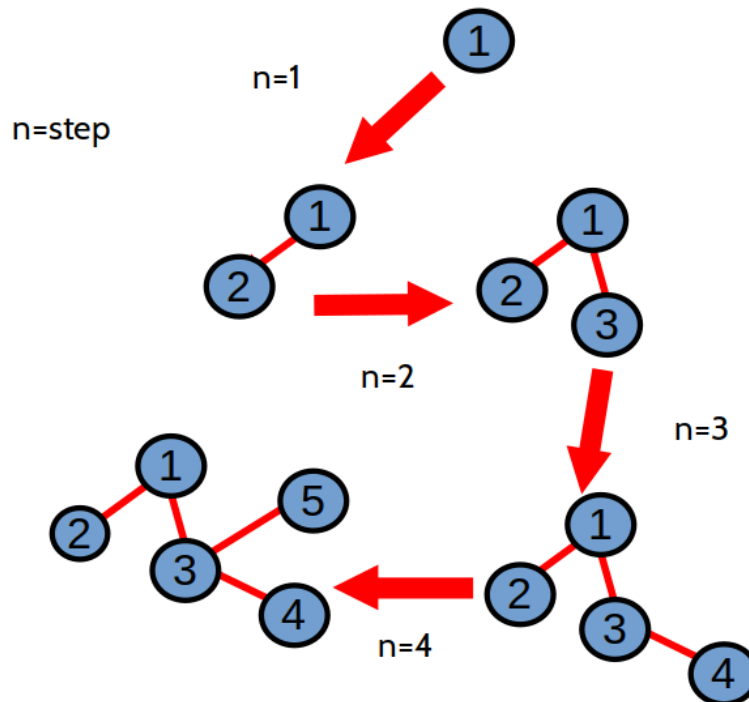


Figure 5. Procedure for building a scale-free network (with 5 nodes). Node 2 is chosen and linked randomly to any other node (say, node 1). Node 3 is chosen next and connected with probabilities $\pi(k_1)$ and $\pi(k_2)$. Node 4 comes next and connected with any of $i=1,2,3$ associated to probabilities $\pi(k_i)$, as expressed in Eq. (1). The process is repeated until all nodes become connected.

2.2.2 The SEIR model implementation

We consider, as a first approximation, that the contagion probability between susceptible individuals and infected ones is p , regardless of whether or not they are relatives. This probability is assumed to be proportional to the contagion rate p_o , as follows:

$$p = p_o \frac{\Delta t}{24hs} \tag{4}$$

where $\Delta t=1$ hour represents the time-step chosen for computing the time evolution of the disease. The time-step remains fixed for all the simulations. The values of p_o are those reported in the literature as typical mean values for the development of the COVID-19 disease (see, for instance, Ref. ³²).

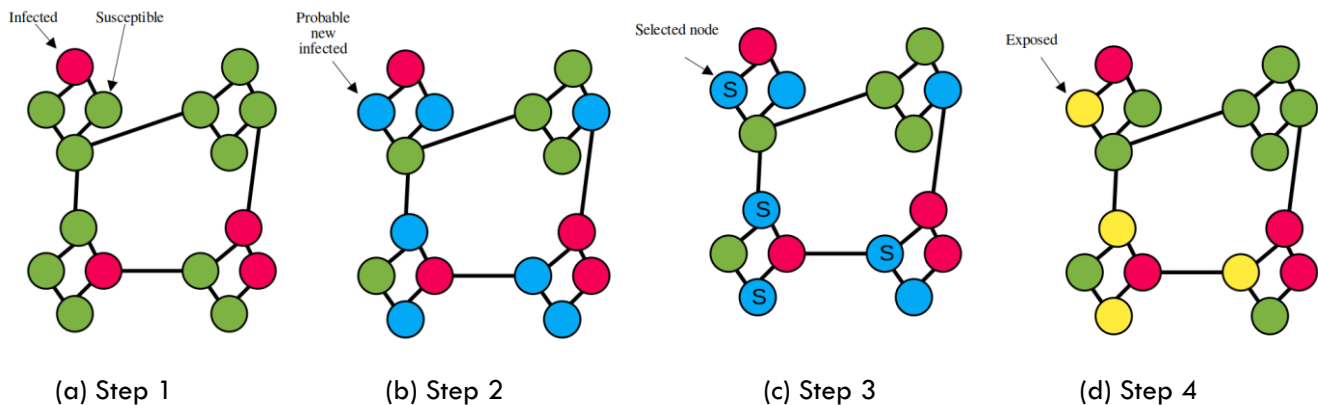


Figure 6. Scheme of the contagion process. The red circles correspond to infected individuals. The green circles correspond to susceptible individuals.

3. Results and Discussion

The results of the investigation are separated into three parts for convenience. The first part deals with those results involving a single community (see Section 3.1). The second part moves to a more complex scenario where two or more communities exist (Section 3.2). The third part compares the single community scenario with the multiple communities scenario, although introducing a slight modification to these networks (for achieving a fair comparison; see Section 3.3).

3.1. RESULTS FOR THE HOMOGENEOUS NETWORK

In this section we present the results obtained when considering a homogeneous network, that is, assuming that there are no local communities (*i.e.* areas of the network more densely connected). The results are divided

We set the initial condition to a single infected individual, chosen at random among the population. The rest of the individuals are set to the susceptible condition. Fig. 6 sketches a few steps after this initial condition. We resume these steps as follows:

1. Identify the infected individuals in the network (see red nodes in Fig. 6a). This is done in no specific order.
2. Any susceptible individual directly linked to an infected one is nominated to become “exposed” with probability p (see Eq.(4)). Susceptible individuals are colored in blue in Fig.6b, and the nominated ones are those labeled with an “S” in Fig.6c.
3. The nominated nodes “S” are then set to the “exposed” stage. These will become infected after the incubation period (see Section 2.1.4).
4. Repeat the above steps until the end of the simulation.

into two steps. We first study the more relevant network characteristics, and secondly, we focus on the spread of the disease on the network with and without the implementation of mitigation strategies.

Fig. 7 shows the degree distributions of random and scale-free networks. Notice from a first examination that the scale-free network achieves very high degree nodes ($k>100$), unlike the random network ($k_{max}\sim 10$). Also notice that the presence of *cliqués* (representing families) does not change significantly the expected *power law* behavior, although the minimum degree for both networks is always four. The scale-free network including *preferential attachment and cliqués* reports a *power law* with exponent $\gamma=-2.82$.

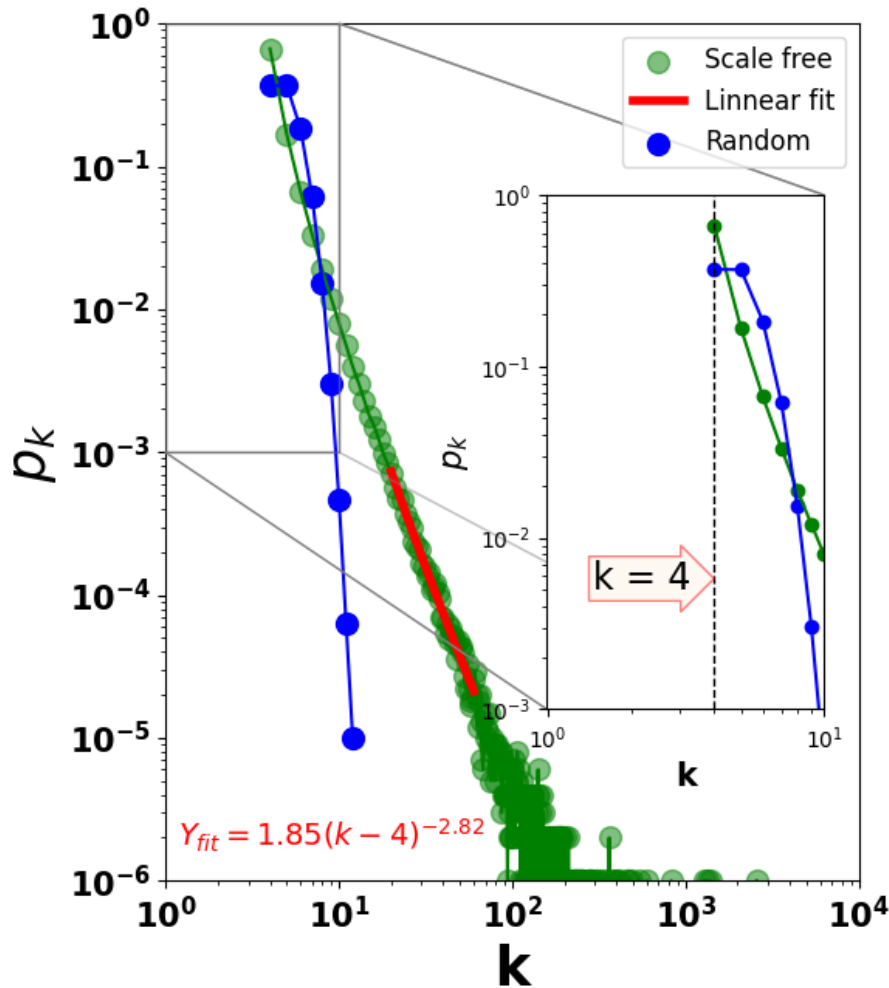


Figure 7. Degree distribution of random and scale-free networks. The red line corresponds to the fitting of the scale-free network (see text for details).

Fig. 8 shows the minimum path distribution for the random and scale-free networks. Both distributions were computed as follows: a node was initially infected and the disease was allowed to propagate throughout the network. We then recorded the time stamps of the rest of

the nodes as they became infected. Thus, we associated the minimum path between one node to any other as the number of “time steps” required for the infection to get to any node from the initial node.

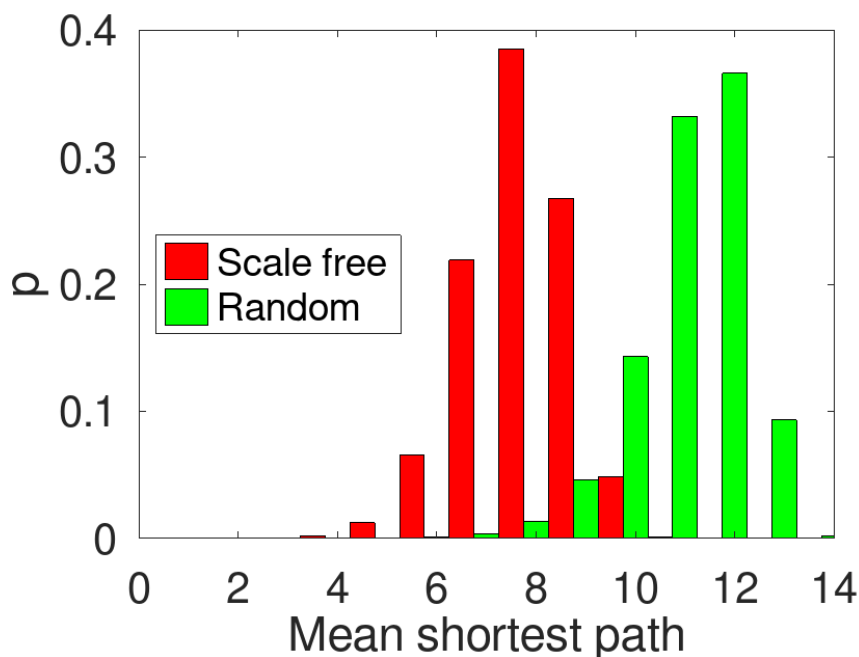
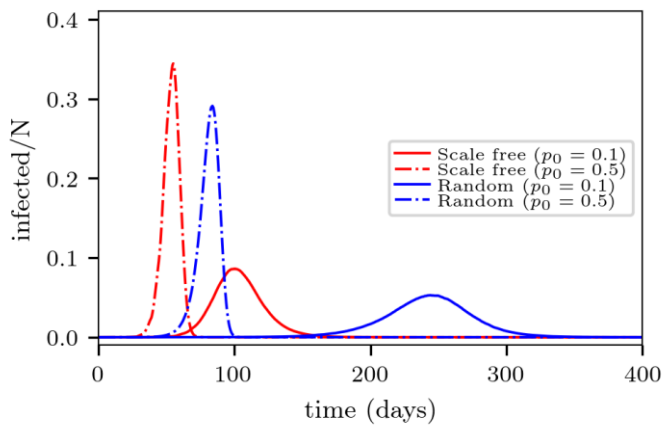


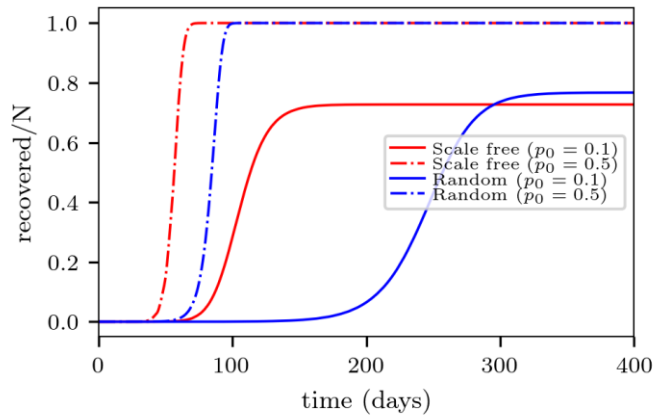
Figure 8. Minimum path distribution for the scale-free and random networks. 50 networks were sampled for each distribution.

It is clear from Fig. 8 that the scale-free network attains smaller mean minimum paths than the random network. Therefore, we can expect that any “infection signal” within the scale-free network will propagate much faster than within the random network.

The next step in the investigation focuses on the disease propagation, but assuming that no containment strategies were available (say, the disease is free to spread in the network). The simulations started by infecting a node at random. We recorded the disease evolution as shown in Fig. 9. It can be seen there the evolution for a single realization, but for two contagion probabilities (see legend for more details).



(a) Infected



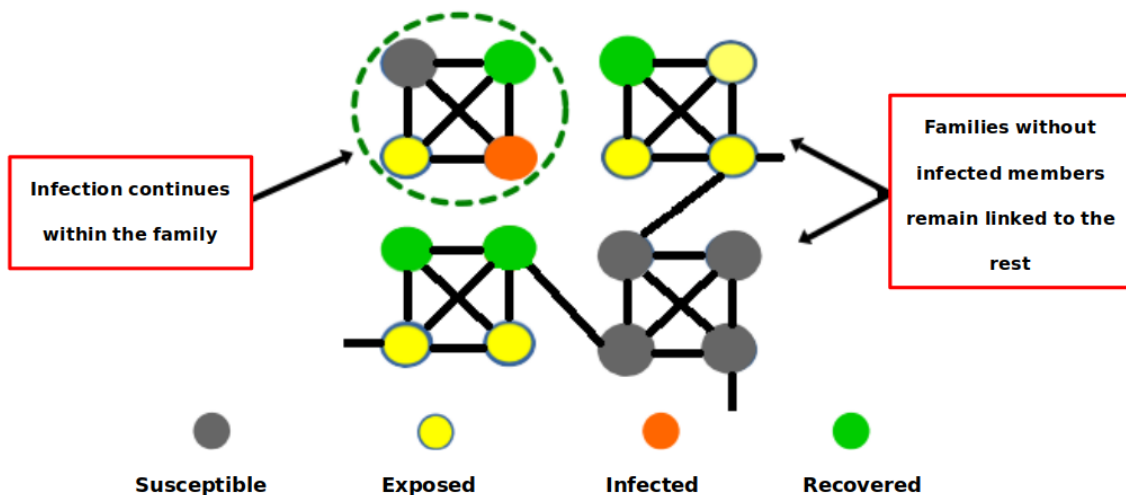
(b) Recovered

Figure 9. The disease evolution for a single realization and two different probabilities ($p_0=0.1$ y $p_0=0.5$, as expressed in Eq. (4)). The blue curves correspond to a random network. The red curves correspond to a scale-free network.

From the inspection of Fig. 9, it is clear that the disease spreads much faster in the scale-free network than in the random network (for similar values of p_0). This is the consequence of the smaller minimum path attained by the scale-free network with respect to the random network. However, this does not mean that the final number of recovered people will be different. We examined these figures and verified that the total number of recovered individuals is similar for both types of networks (with similar values of p_0). Thus, the dynamics of the disease spreading depends strongly on the kind of network, but we may expect similar figures at the end of the epidemic. We next proceeded to study the “performance” of random and scale-free networks under containment actions. These actions, however, do not consider

pharmacological actions (i.e. application of vaccines). Two alternative strategies were analyzed: the family isolation and the individual isolation. The main features are detailed below:

1. **Family isolation:** an entire family is isolated from the rest of the people (neighbors, friends, etc.) if at least one member of the family is infected (see Fig. 10a). This stage remains unchanged until no other member of the family gets infected.
2. **Individual isolation:** all infected individuals are isolated from both their family and the rest of the people (neighbors, friends, etc.; see Fig. 10b). This stage remains unchanged until the individual recovers.



(a) Family isolation

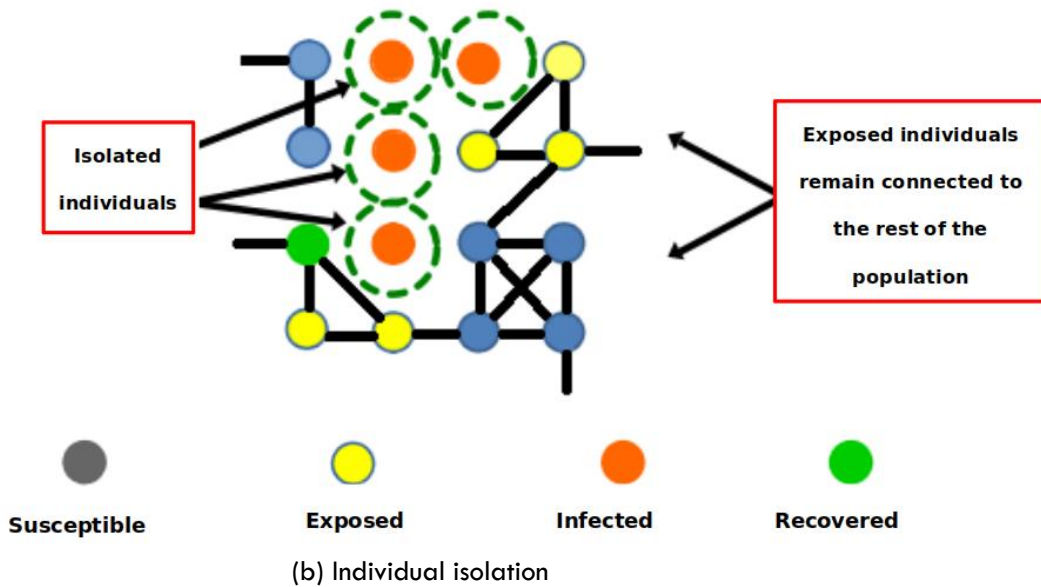


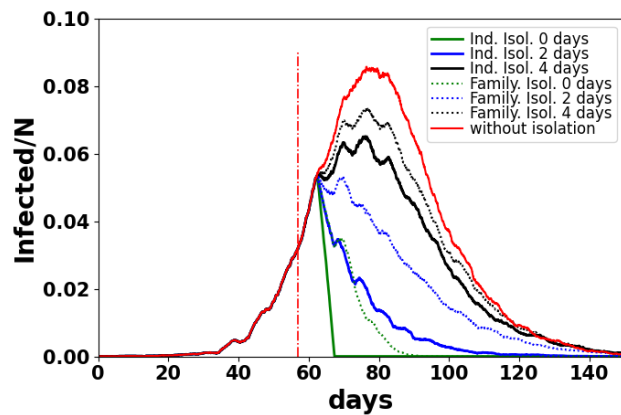
Figure 10. Scheme for two containment actions, as explained in the text.

We stress that our simulations considers real life delays due to epidemiological tests (say, the time required for processing blood, spittle, etc.). We assumed that any action was implemented after D days of getting the infection. For instance, a family or an infected person is isolated from the rest of the people after D days of infected.

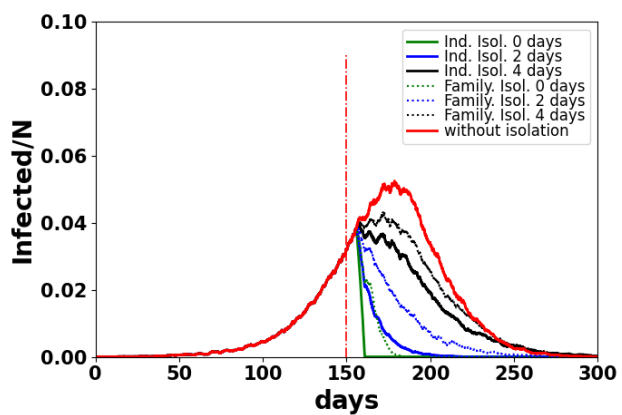
Fig. 11 compares both isolation strategies on homogeneous networks, implemented just after 5000 people got infected. Notice that the most effective strategy to reduce the number of infected people on both networks (random and scale-free) corresponds to the isolation of individuals from the rest of the people (even

the family). However, the delays in the epidemiological tests affect both types of strategies in a similar way.

The results in Fig. 11 are a strong warning on the clinical tests delays: any delay surpassing 4 days reduces significantly the efficiency of the strategy. That is, we may expect results almost similar to those without actions at all (red curve in Fig. 11). This can be explained by comparing the testing delays with the time period of the infection (5 days). The isolation action becomes spoiled whenever the infected individual remains non-isolated during almost the entire infection (while waiting for the clinical tests).



(a) Scale-free



(b) Random

Figure 11. Infection curves with containment actions. The “family isolation” strategy is represented in dashed lines for all the analyzed delays. The “individual isolation” strategy is represented in solid lines for all the analyzed delays. The contagion probability is $p_0=0.1$. The vertical line in red corresponds to the beginning of the isolation strategy (see text for details).

The main conclusion that comes up from the above results is that individual isolation appears as the most effective strategy for reducing the spread of the disease, although the family isolation also arrives to quite positive results. However, the delays in test reports produce a negative impact on the mitigation of the disease. An early isolating of the infected individual is therefore the most desirable situation, no matter if the contagion is random-like or scale-free.

3.2 RESULTS FOR THE HETEROGENEOUS NETWORK

So far we have analyzed how the epidemic evolves in an homogeneous network. Now, we focus on how these results change in the presence of communities, that is, when groups of individuals are more densely connected among them than with respect to the rest of the city.

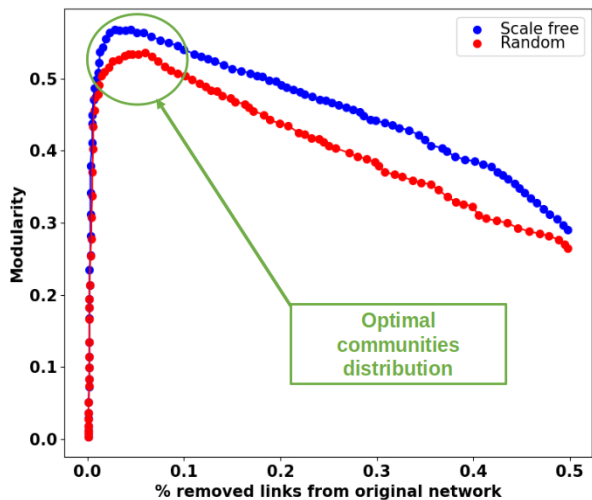
As mentioned in Section 2.1, we implemented the Girvan-Newman algorithm for detecting communities within a

network. Recall that this algorithm starts from a homogeneous network and successively eliminates those links with greater *betweenness* until C isolated sub-graphs are obtained.

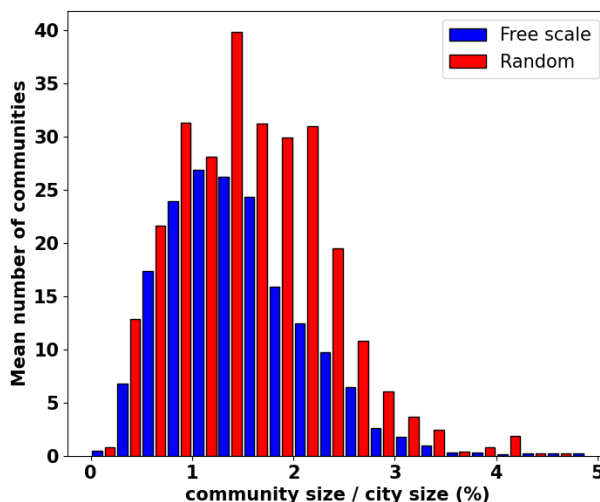
Fig. 12a shows the average *modularity* as a function of the number of links removed in each kind of network. Notice that the maximum *modularity* occurs after removing approximately 5% of the total links with the highest *betweenness*. This is the optimum detection of communities that we can achieve for either the random

and the scale-free networks. We will limit our investigation to this scenario.

The detection process identified approximately 70 communities. Fig. 12b shows the size distribution of these communities. As can be seen, the largest community includes approximately 5% of the total nodes of the network, regardless of the explored network. This corresponds to approximately 250 individuals in the simulated networks. We will refer to this community as “the neighborhood” or simply “neighborhood” from now on.



(a) Modularity



(b) Size of the communities

Figure 12. (a) Modularity as a function of the fraction of removed links from the original network (expressed in percentage; see text for details). The sample corresponds to 25 network realizations of each kind (random and scale-free). The size of the realization was $N=5000$. (b) Size distribution of the communities at the optimum detection point (see text for details).

We next explored the distribution of the minimum path for “the neighborhood” (i.e. largest community) and the rest of the city. Both distributions were computed by first isolating one from the other, and then proceeding to compute the minimum path separately for each sub-network (see Fig.13).

A noticeable feature in the networks shown in Fig. 13 is that the distributions for “the neighborhood” are somehow wider than the distributions of the city. Thus, the neighborhood appears as a more heterogeneous area in terms of minimum path compared to the rest of the city.

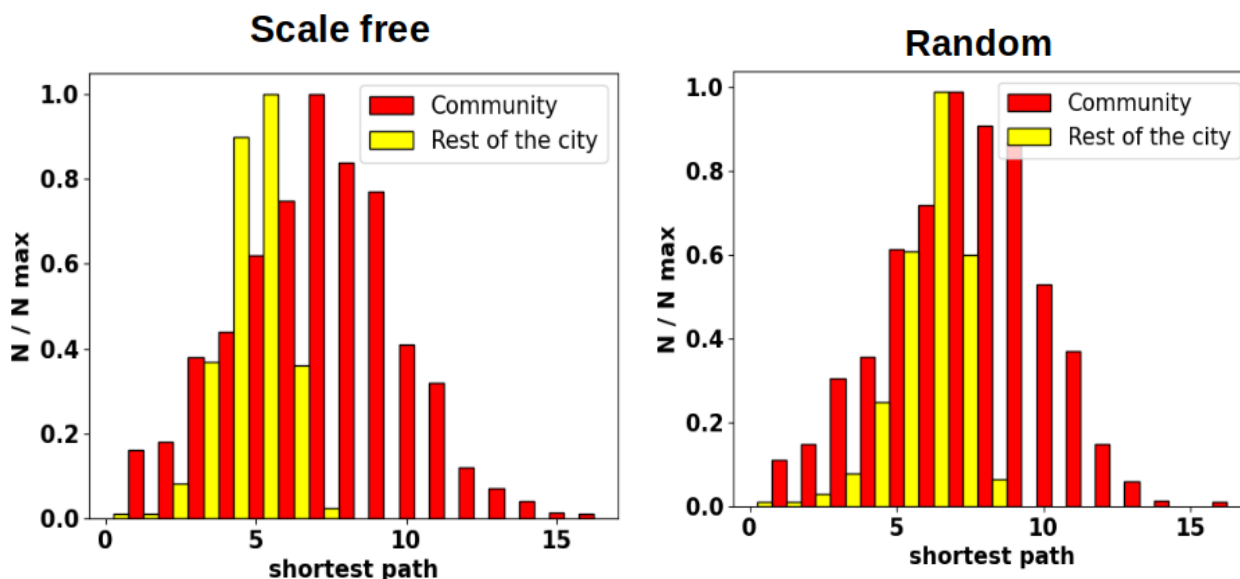


Figure 13. Minimum path distribution for “the neighborhood” and the rest of the city (see legend for details).

We are actually not interested in a “neighborhood” achieving long paths, but those where the disease spreads easily. This means that our target corresponds to the “neighborhoods” standing on the left-most part of the distribution in Fig. 13. These represent very densely connected “neighborhoods”, so we decided to bias the “neighborhood” by increasing its links. We proceeded as follows: we kept unchanged the current links of the “neighborhood” (for either the random and the scale-free networks), but further linked these nodes with additional random links. The number of new links was the same as

the number of old ones (say, the total number was twice the one for the original “neighborhood”).

Fig. 14 shows the minimum path distribution for the “crowded neighborhood” (attaining twice the original connectivity) and the rest of the city (unchanged). The former is now located on the left of the plot, as expected. Complementary, Fig. 15 provides a visual impression of the “crowded neighborhood” and the rest of the city (see caption for details).

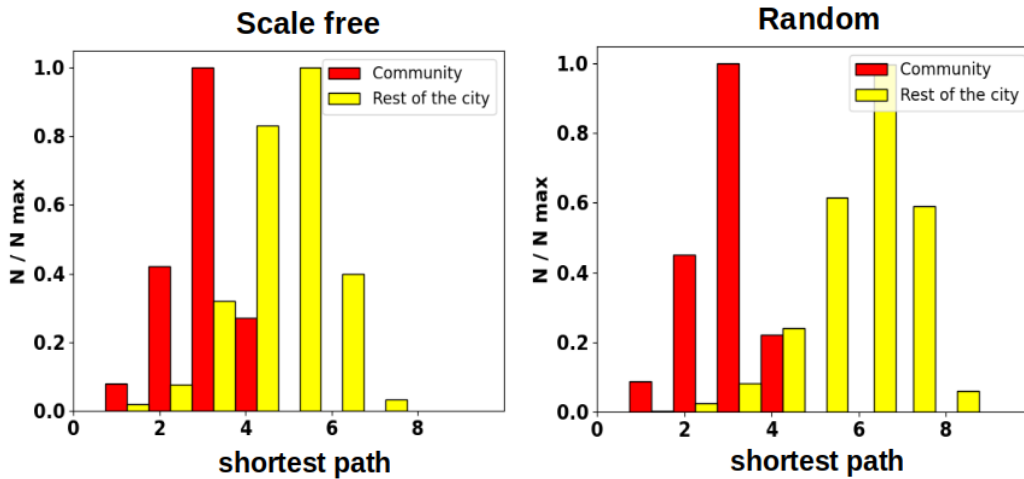


Figure 14. Minimum path distribution for the “crowded neighborhood” and the rest of the city (see legend for details).

Two remarkable features appear in Fig. 15: (i) the “crowded neighborhood” corresponds to the region with the highest degree in the network (for both types of networks), and, (ii) the scale-free network presents hubs

as the one highlighted in the top-center picture. In turn, the random network presents a more homogeneous degree compared to the scale-free one.

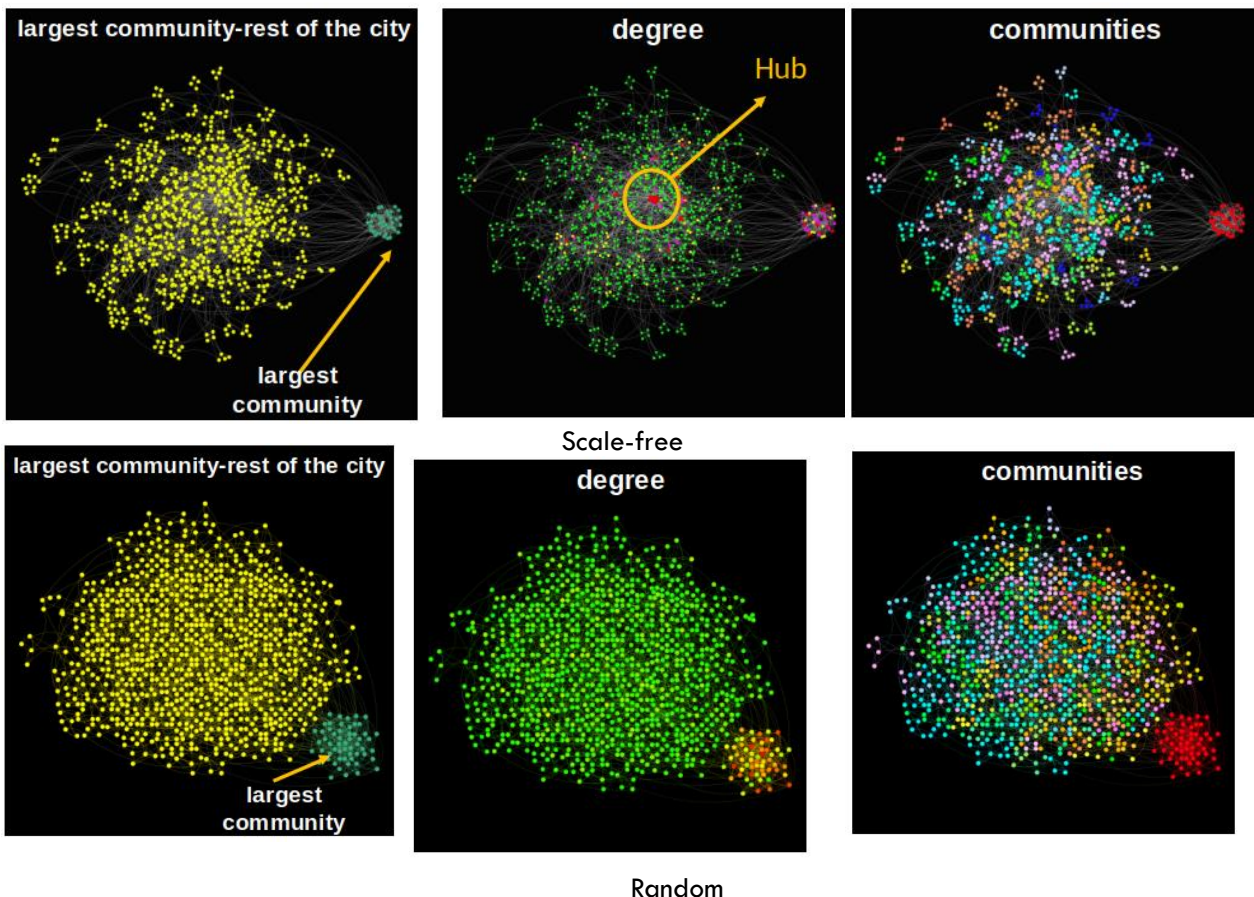


Figure 15. Visual representation of the “crowded neighborhood” and the rest of the city. Column on the left: nodes and links of the “crowded neighborhood” (blue) and the rest of the city (yellow). Column at the center: degree of the nodes (greenish tones associated with low degree and reddish tones associated with high degree). Column on the right: communities within the city, identified by colors. Top row: scale-free network. Bottom row: random network.

The next step of the investigation moves to the analysis of the disease spreading in the presence of communities. We followed the same procedure as in Section 3.1: a node belonging to the city, but outside the “crowded neighborhood”, gets infected and the disease propagates freely throughout the network. The time evolution of the infection is shown in Fig. 16 (see caption for details). Notice that the disease spreads faster in the “crowded neighborhood” than in the rest of the city. This is quite a drawback for this community since once the disease reaches the community, it soon gets infected due to the short paths among people.

In order to avoid a massive contagion in the “crowded neighborhood”, our first intention might be to isolate this community from the rest of the city. We proceed this way in our simulations. We cut-off the links connecting the community to the rest of the city after some time from the beginning of the contagion (not shown). We observed that this isolation action only prevents the entry of the disease to the “crowded neighborhood”, but once it enters, the dynamic of the contagion follows a similar pattern as the one depicted in Fig. 16.

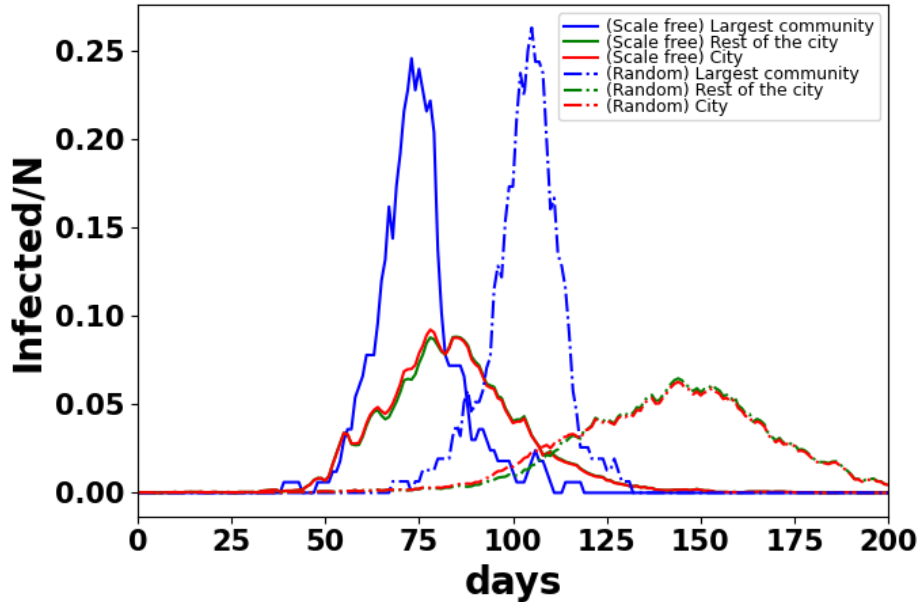


Figure 16. The disease evolution in the random and scale-free networks (see legend). The number of infected people is normalized by the total population $N=5000$ individuals. The contagion probability is $p_0=0.1$. 50 networks of each kind were sampled.

We conclude from this Section that the detection of crowded communities is a major issue in the planning containment actions. These may increase significantly the spreading speed of the disease. A safe strategy should allow quick actions on the links connecting crowded neighborhoods to the rest of the city.

3.3 RESULTS FOR THE MIXED NETWORK

Recall that in the previous Section, we added links to the “crowded neighborhood” to simulate a crowded community. This means the city with a crowded community has n extra (random) links with respect to the homogeneous network. Thus, the comparison of the

epidemic “performance” between both networks is not straightforward. A fair comparison requires the same number of links in both networks. This Section deals with this matter.

Our aim is to increase the number of links of any of the networks presented in Section 3.1 for the comparison to networks in Section 3.2. The simplest way to do this is to randomly add the necessary links, no matter if the network is random or scale-free. That is, links are added among *all* the nodes in the homogeneous network. We will call this new network a “mixed” or “hybrid” network and a scheme is shown in Fig. 17.

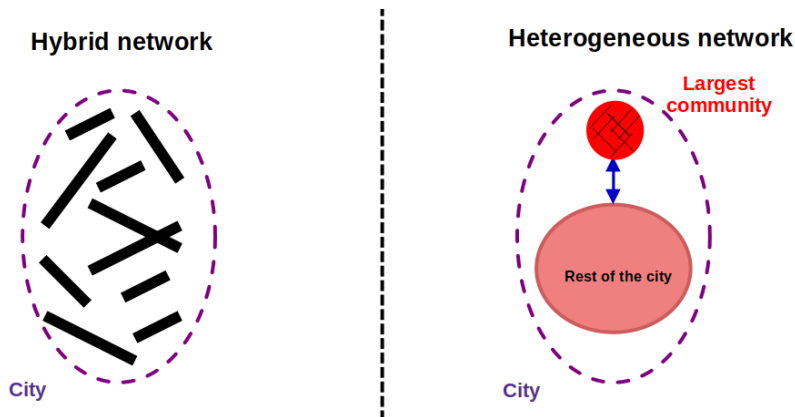
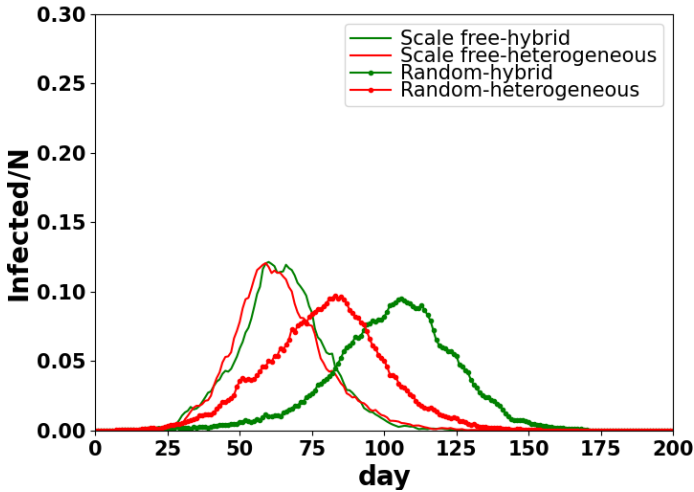


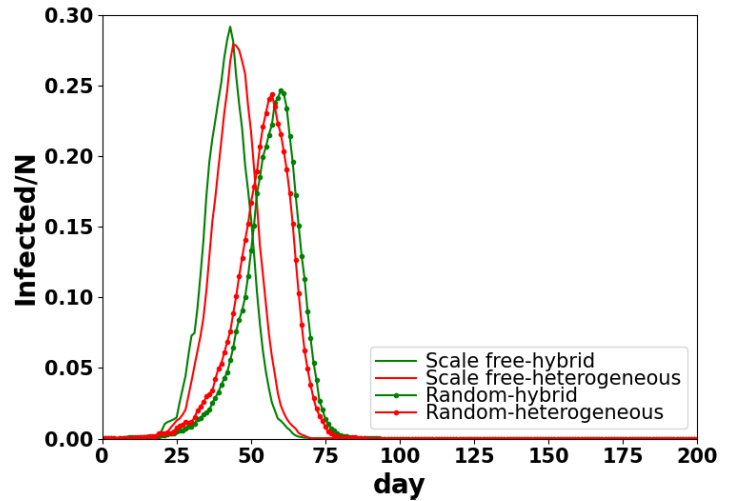
Figure 17. Schematic representation of a heterogeneous network (Section 3.2) and a hybrid network (see text for details). The black lines on the right correspond to the new (random) links added to homogeneous networks (Section 3.1).

Fig. 18 shows the time evolution of the epidemic for networks attaining a “crowded neighborhood” and mixed networks. Two contagion probabilities are explored in there, $\rho_o=0.1$ and $\rho_o=0.3$, respectively. Notice that no

significant differences between homogeneous and heterogeneous (with a crowded community) can be observed for $\rho_o=0.3$. Thus, this case is not relevant from the point of view of the mixed network.



(a) $\rho_o=0.1$



(b) $\rho_o=0.3$

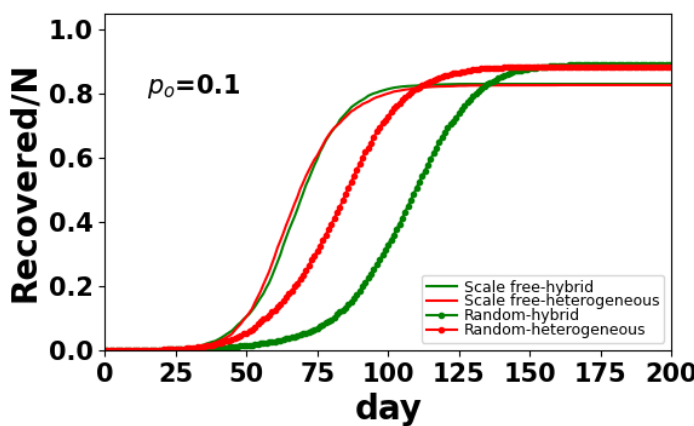
Figure 18. The disease evolution for the heterogeneous networks and the mixed networks (see text for details). 50 networks of each kind were sampled.

The situation for $\rho_o=0.1$ is the most interesting case. Two behaviors can be distinguished: (i) in the random network environment, the presence of a crowded neighborhood speeds-up the disease propagation with respect to the mixed network, as expected. (ii) in the scale-free environment, the disease propagation is similar, although the presence of a crowded neighborhood.

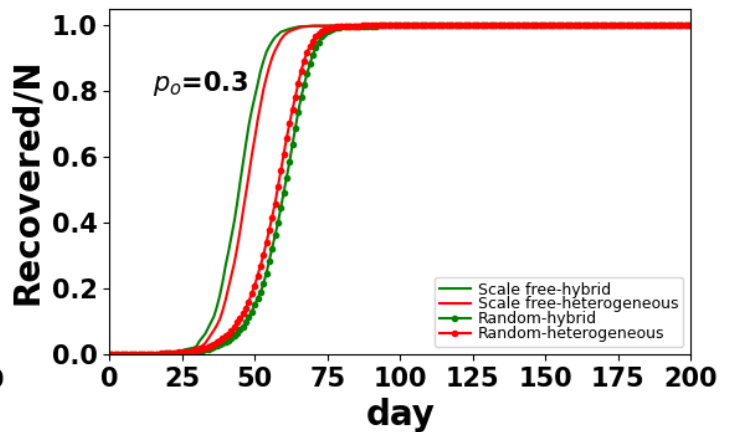
Notice that the above dynamics are relevant at $\rho_o=0.1$. But, at $\rho_o=0.3$ the disease evolution appears quite independent of whether there exist *hubs* or crowded communities.

The behavior (ii) is somehow puzzling. A closer inspection of the propagation dynamic shows that the presence of *hubs* is of major relevance. These provide the means for speeding-up the disease propagation, not only in the crowded neighborhood but in all the city.

Fig. 19 exhibits the fraction of recovered people for heterogeneous and mixed networks. The plots confirm that the kind of network (heterogeneous or mixed) only affects the speed of the propagation of the disease, but not the final number of infected people.



(a) $\rho_o=0.1$



(b) $\rho_o=0.3$

Figure 19. Fraction of recovered people as a function of time for the heterogeneous networks and the mixed networks (see text for details). 50 networks of each kind were sampled.

4. Conclusions

The investigation studies the spatial-temporal evolution of an infection (COVID-19) from a microscopic point of view. Individuals are represented as nodes linked to each other in a complex network. Links may occur with a fixed probability for all the nodes, or, with varying probability

from one node to another. The former constitutes a random network and the latter a scale-free network.

We explored homogeneous networks (single community) and heterogeneous ones (many communities). In any case, we included the family structure in the description.

Besides, the epidemiological model within the network was always assumed to be a SEIR-like model.

We arrived to the following conclusions:

- (a) In the homogeneous context, the scale-free network speeds-up the disease propagation with respect to the random network. This occurs because of the smaller minimum path in the scale-free network. Also, the infection lasts longer in the random network than in the scale-free network. The containment actions consisted of isolating the infected individual, or, her/his complete family from the rest of the population. We concluded that it is more effective to isolate the individual since an early detection of the disease prevents the rest of the family from becoming infected, and likewise, prevents further spreading. However, clinical tests delays reduce significantly the efficiency of the strategy. This is a strong warning for the implementation of containment actions.
- (b) In the heterogeneous context, the investigation showed that a crowded neighborhood speeds-up the

disease propagation from the time the infection enters this neighborhood. Actions on the links between the crowded neighborhood and the rest of the city should be taken as quick as possible.

We ended the investigation by comparing the homogeneous and heterogeneous contexts. Care was taken to make a fair comparison by means of modified networks with a similar number of links. We arrived to the conclusion that crowded neighborhoods or *hubs* are relevant if the contagion probability is low ($p_0 \approx 0.1$). However, for higher probabilities ($p_0 \approx 0.3$) these are not relevant at all in the propagation speed.

Acknowledgments

C.O. Dorso is Superior Researcher at Consejo Nacional de Investigaciones Científicas y Técnicas (CONICET) and Chief Prof. at Depto. de Física-FCEN-UBA. G.A. Frank is Adjoin Researcher at CONICET. F.E. Cornes is PhD researcher at FCEN-UBA and H.E. Benitez has degree in Physics at FCEN-UBA.

References

1. C. Heine, K. O’Keeffe, P. Santi, Travel distance, frequency of return, and the spread of disease, *Sci Rep.* 13, 14064 (2023).
2. A. Medus, C. Dorso, Diseases spreading through individual based models with realistic mobility patterns., *arXiv:1104.4913 [q-bio.PE]* (2011).
3. S. E. Eikenberry, M. Mancuso, E. Iboi, T. Phan, K. Eikenberry, Y. Kuang, E. Kostelich, A. B. Gumel, To mask or not to mask: Modeling the potential for face mask use by the general public to curtail the covid-19 pandemic, *Infectious Disease Modelling* 5, 293-308 (2020).
4. X. Zhang, Y. Song, H. Wanga, G.-P. Jiang, Epidemic spreading combined with age and region in complex networks, *Hindawi Mathematical Problems in Engineering* 5 (2020).
5. D. Barmak, C. Dorso, M. Otero, Modelling dengue epidemic with human mobility, *Physica A* 47 129-140 (2016).
6. F. Cornes, G. Frank, C. Dorso, Covid-19 spreading under containment actions, *Physica A: Statistical Mechanics and its Applications* 588, 126566 (2022).
7. F. Cornes, G. Frank, C. Dorso, Estrategia ciclica de aislamiento y actividad económica durante la pandemia covid-19., *Anales AFA* 31(4) (2021).
8. Y. M. Bar-On, A. Flamholz, R. Phillips, R. Milo, Science forum: Sars-cov-2 (covid-19) by the numbers, *eLife* 9, e57309 (2020).
9. R. Li, S. Pei, B. Chen, Y. Song, T. Zhang, W. Yang, J. Shaman, Substantial undocumented infection facilitates the rapid dissemination of novel coronavirus (covid-19), *medRxiv* (2020).
10. J. Read, J. Bridgen, D. Cummings, A. Ho, C. Jewell, Novel coronavirus 2019-ncov: early estimation of epidemiological parameters and epidemic predictions, *Philosophical Transactions of the Royal Society b: Biological Sciences* 376, 376 (2021).
11. A. J. Kucharski, T. W. Russell, C. Diamond, Y. Liu, C. nCoV working group, J. Edmunds, S. Funk, R. M. Eggo, Early dynamics of transmission and control of covid-19: a mathematical modelling study, *medRxiv* (2020).
12. X.-Y. Yan, C. Zhao, Y. Fan, Z. Di, W.-X. Wang, Universal predictability of mobility patterns in cities, *Journal of The Royal Society Interface* 11 (2013).
13. D. Brockmann, L. Hufnagel, T. Geisel, The scaling laws of human travel., *Nature* 439, 462-465 (2006).
14. M. González, C. Hidalgo, A. Barabási, Understanding individual human mobility patterns, *Nature* 453, 779-782 (2008).
15. I. Rhee, M. Shin, S. Hong, K. Lee, S. Chong, On the levy-walk nature of human mobility., *IEEE INFOCOM 2008 - The 27th Conference on Computer Communications*, Phoenix, AZ, USA. 924-932 (2008).
16. M. Ahsanullah, V. Nevzorov, Some inferences on the levy distribution., *Journal of Statistical Theory and Applications* 13(3) 205-211 (2014).
17. I. A. Perez, M. A. Di Muro, C. E. La Rocca, L. A. Braunstein, Disease spreading with social distancing: A prevention strategy in disordered multiplex networks, *Phys. Rev. E* 102 022310 (2020).
18. L. Valdez, L. Braunstein, S. Havlin, Epidemic spreading on modular networks: The fear to declare a pandemic., *Phys. Rev. E.* 101 032309 (2020).
19. M. Kuperman, G. Abramson, Small world effect in an epidemiological model., *Phys. Rev. Lett.* 86, 2909 (2001).
20. H. Wearing, M. P. Rohani, Appropriate models for the management of infectious diseases., *PloS Medicine* 2(7) 0621–0627 (2005).
21. P. Erdős, A. Rényi, On random graphs, *Publ. Math. Debrecen* 6 290-297 (1959).
22. A.-L. Barabási, R. Albert., Emergence of scaling in random networks., *Science* 286 509-512 (1999).
23. Albert, L. Barabási, *Network Science* 1st Edition, Cambridge University Press, (2016).
24. A.-L. Barabási, E. Bonabeau, Scale-free networks., *Scientific American* 208(5) 60-69 (2003).
25. M. Newman, Fast algorithm for detecting community structure in networks, *Phys. Rev. E.* 69, 066133 (2004).
26. M. van den Heuvel, O. Sporns, Network hubs in the human brain., *Trends in Cognitive Sciences* 12(12) 683-696 (2013).
27. M. Saberi, R. Khosrowabadi, A. Khatibi, B. Misic, G. Jafari, Topological impact of negative links on the stability of resting-state brain network, *Scientific Reports* 11(1) 269-271 (2021).
28. S. Perera, M. Bell, M. Bliemer, Network science approach to modelling the topology and robustness of supply chain networks: a review and perspective, *Applied Network Science* 2, 33 (2017).
29. D. Watts, S. Strogatz, A social network model based on caveman network, *Nature* 393(6684) 440-442 (1998).
30. A. Medus, C. Dorso, Alternative approach to community detection in networks., *Phys. Rev. E.* 79(6) 066111 (2009).
31. M. Girvan, M.E.J. Newman, Community structure in social and biological networks., *Proc. Natl. Acad. Sci. USA.* 99 7821–7826 (2002).
32. Y. Wu, L. Kang, Z. Guo, J. Liu, M. Liu, W. Liang, Incubation period of covid-19 caused by unique sars-cov-2 strains: A systematic review and meta-analysis., *JAMA Netw Open* 5(8) e2228008 (2022).